ELSEVIER

Polymer 43 (2002) 621–628

polymer

www.elsevier.com/locate/polymer

Modeling of poly(isoprene) melts on different scales ☆

Roland Faller*, Florian Müller-Plathe

Max-Planck-Institut für Polymerforschung, Ackermannweg 10, 55128 Mainz, Germany

Abstract

Atomistic (atom-scale) and coarse-grained (meso-scale) simulations of the structure and dynamics of poly-isoprene melts are compared. The local structure and chain packing is mainly determined by the atomistic details of the polymer architecture. The large-time dynamics encountered in NMR experiments can be explained by meso-scale simulations including stiffness. The connecting link between the two scales is the stiffness which, although being a local property, influences strongly even the long-timescale dynamics. The standard reptation scenario fails to explain the observed dynamics. We propose *strong reptation* as a modified reptation scenario in which the local Rouse motion is absent.

Keywords: Poly-isoprene; Modeling; Molecular dynamics

1. Introduction

The large abundance of polymers and their variety of applications make them an interesting target of study in theoretical material science. The understanding of the differences and similarities of the various materials is an important prerequisite for the goal of CAMD — computer aided materials design. The dream of chemical engineers would be to develop in the workstation the perfect material for a given purpose.

To come closer to this distant goal, much effort in various fields is necessary. As polymeric materials are characterized by the importance of various length scales, the understanding of the interplay between these scales is of utmost importance. Methods adapted to all relevant scales are needed from the experimental as well as from the theoretical or simulational viewpoint. In simulations, much work has been directed recently towards the issue of *coarse-graining*, the mapping of simulations on different scales, in order to achieve a unified view of the arising scales [1–5]. In the present contribution, we show that atomistic simulations of *trans*-polyisoprene (PI) [6] can be mapped onto a simple bead-spring model incorporating excluded volume, connectivity, and stiffness [7,8]. With this simple model we can investigate the long-time dynamics of chains in the melt. There is evidence for reptation which qualitatively changes with stiffness [9,10]. This connects to some results of modern NMR experiments [11] which we can reproduce to a satisfactory extent [8,12]. Thus, simulations on both scales and especially their connection reveal different important aspects of the system under study.

The remainder of this contribution is organized as follows. In Section 2, a short review about our recent results of atomistic simulations of *trans*-PI is given. In Section 3, results of simulations on the meso-scale level, where the polymer identity is put into a simple stiffness parameter, are presented. In the concluding section, the importance of chain stiffness is discussed. We show that matching chain stiffness is sufficient to allow a mapping for the poly-isoprene models presented here.

2. Local structure and dynamics — the atomistic scale

The atomistic structure of oligomers of *trans*-1,4-poly-isoprene (cf. Fig. 1) was investigated. For details of the simulations and the interaction potentials see Refs. [6,9]. Here we only note that the simulation box contains 100 oligomers of average length 10 monomers of pure *trans*-poly-isoprene which were pre-equilibrated using end-bridging Monte Carlo [13,14] at the ambient condition of 300 K or the elevated temperature of 413 K. All atomistic simulations are run at 101.3 kPa.

The main result is, that the local structure is very important for properties on the sub-monomer length scale. Fig. 2

☆ This paper was originally submitted to *Computational and Theoretical Polymer Science*. Following the incorporation of *Computational and Theoretical Polymer Science* into *Polymer*, this paper was consequently accepted for publication in *Polymer*.

* Corresponding author. Present address: Department of Chemical Engineering, University of Wisconsin-Madison, 1415 Engineering Drive, Madison, WI 53706-1691, USA. Tel.: +1-608-262-3370; fax: +1-608-262-5434.

E-mail address: faller@che.wisc.edu (R. Faller).

0032-3861/02/$ - see front matter
PII: S1089-3156(01)00013-7

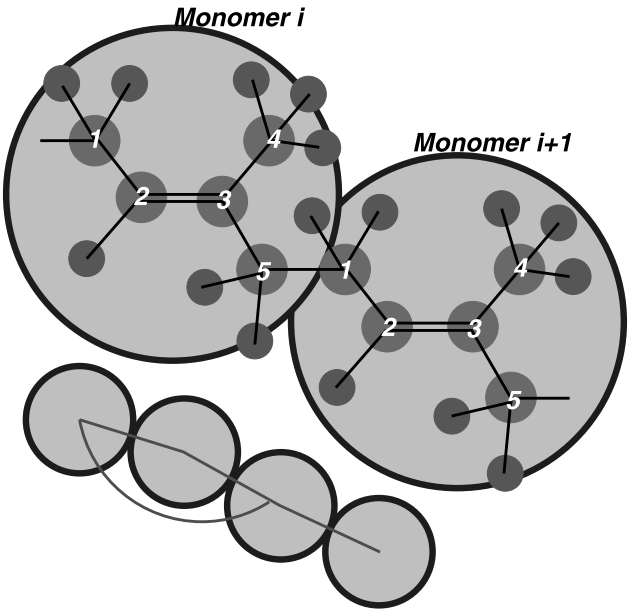

Fig. 1. The atomistic structure of *trans*-1,4-poly-isoprene and its mapping to a bead-spring model including only excluded volume and stiffness.

shows the local mutual packing of chains by means of radial distribution functions of the different atoms in the melt. The carbon atoms show a distinct peak at next neighbor contact. The hydrogen atoms, in contrast, show very little structure. Thus, we encounter a carbon backbone with a surrounding 'hydrogen cloud'. This can be taken as a first hint that not all details are necessary for every simulation. Still, the hydrogen atoms must be taken into account for the C–H vector reorientation. This is important for direct comparison to NMR experiments (below). The comparison to experimental raw data is always a good and necessary validation of simulation models [12].

The local packing is additionally reflected by the directionality of chains at contact. This is shown in Fig. 3 by means of the spatial orientation correlation function of the double bonds

$$\mathrm{OCF}(r) := P_2(r) = \left\langle \frac{1}{2}[3\cos^2\alpha(r) - 1] \right\rangle, \tag{1}$$

where $\alpha(r)$ is the angle between tangent unit vectors on two different chains. The distance r is measured between their centers of mass. The unit vectors may be defined in different manners, e.g. the direction vector along double bonds in Fig. 3 is one possibility to denote the direction of a monomer.

Direct comparisons to experiments [15–17] and simulations [18,19] on *cis*-polyisoprene prove that our model is realistic [6,9].

The reorientation of the carbon–hydrogen vectors is subject to a two-stage process (cf. Fig. 4). The first stage is a fast initial decay on the time-scale of the segmental motion, i.e. the motion on the monomer or sub-monomer scale. In the second reorientation stage, the reorientation of the whole oligomer shines through. Overall, reorientation is

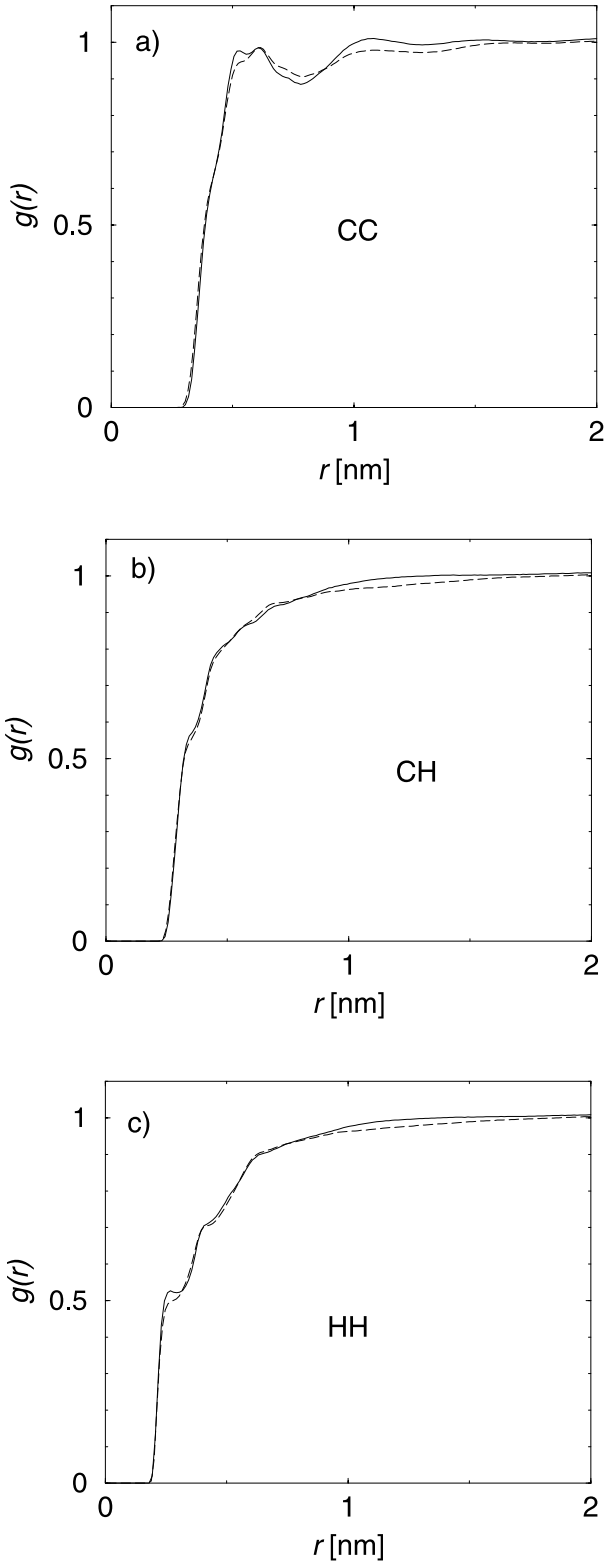

Fig. 2. Radial distribution functions of atomistic data of *trans*-polysoprene. (a) Carbon–Carbon, (b) Carbon–Hydrogen, and (c) Hydrogen–Hydrogen RDFs. The carbons show a stronger pronounced structure. A correlation hole can be seen in subfigure (c).

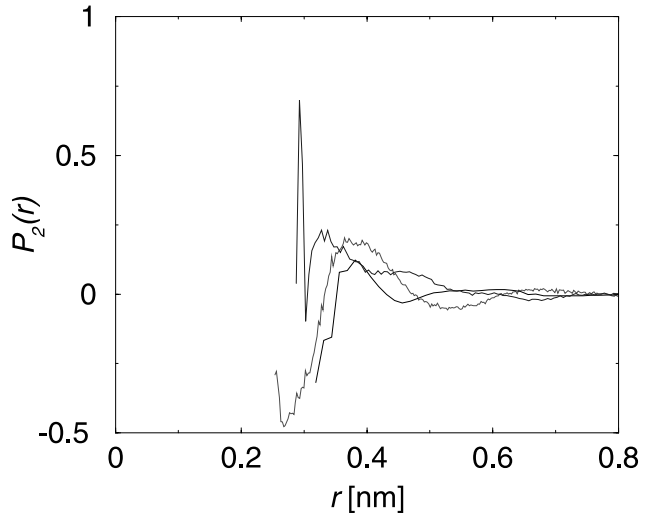

Fig. 3. Atomistic mutual orientation (OCF(r)) of double-bonds (dotted) in *trans*-polyisoprene in comparison to the fully flexible simple model of Section 3 (solid). The dashed line is for the atomistic vectors connecting C_5 with C_1 of the next monomer.

monitored by the following correlation function:

$$C_{\text{reor}} = \left\langle \frac{1}{2}[3\cos^2\Phi(t) - 1] \right\rangle. \tag{2}$$

Here, $\Phi(t)$ is the angle by which a given bond vector reoriented in time t. The second Legendre polynomial is chosen because it is the relevant quantity in NMR measurements. The effectiveness of the two stages may be measured by fitting double exponential decays to the obtained correlation functions. In doing so, satisfactory agreement with experiments could be achieved (cf. Table 1) if we keep in mind that the investigated systems are not completely identical. The experiments were performed on mixtures with a high *cis*-PI content and longer chains.

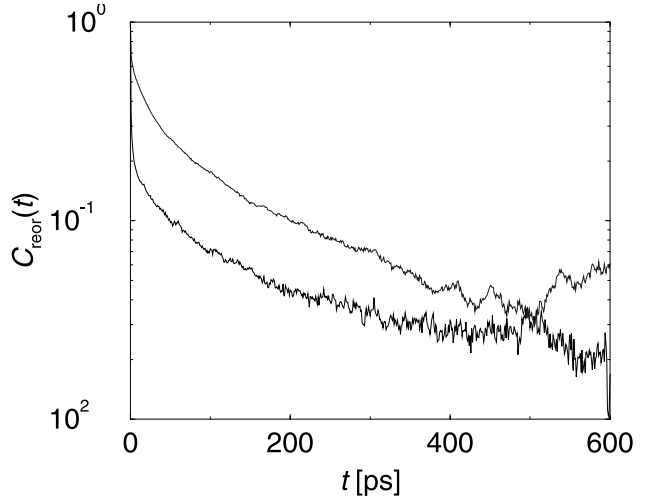

Fig. 4. Reorientation correlation functions of the methylene C–H vectors at 413 K. Upper: C_5–H, Lower: C_1–H.

Table 1
Comparison of the experimental (*cis*-PI) and simulation (*cis* and *trans*-PI) data for the efficiency of the initial stage of the reorientation process. The parameter a denotes to which value the reorientation correlation function (Eq. (2)) decays in the short-time process, i.e. before the long-term exponential relaxation sets in. $a_{1\text{ps}}$ is the value of $1 - C_{\text{reor}}$ at 1 ps. In the analysis of the simulations for *cis*-polyisoprene a stretched exponential second process was assumed. The experiments used a range of temperature between 283 and 363 K [15]. The *trans* simulations were at 300 K [6] and the *cis* simulations at 363 K [19]

Vector	$a_{1\text{ps}}^{trans}$	a_{sim}^{cis}	a_{Exp}^{cis}
	Sim.: this work	Sim.: Ref. [19]	exp: Ref. [15]
C_1–H	0.42	0.28	0.40
C_2–H	0.16	0.16	0.17
C_5–H	0.18	0.23	0.48

In Section 3.2, comparisons of the long-time dynamics of the corresponding simple model with experiments will be presented.

3. Global structure and dynamics — meso-scale simulations

Simple polymer models allow one to investigate large-scale phenomena both in time and space which are not accessible by atomistic simulations. Therefore many researchers employ such models to look for rather generic polymer properties or dynamical concepts [20–25]. One of these important concepts is reptation [26,27]. The reptation concept explains much of the molecular weight dependence of viscosity and the elastic and loss moduli [27]. However, this model originates from the simple Rouse model [28] where no stiffness is included or it is subsumed into simple *Kuhn blobs* [29].

In order to look for the influence of stiffness, a three-body potential for stiffening the backbone has been introduced [7,8,30]

$$\frac{V_{\text{angle}}}{k_{\text{B}}T} = \frac{l_{\text{p}}}{k_{\text{B}}T}[1 - \vec{u}_i \cdot \vec{u}_{i+1}]. \tag{3}$$

The angle force constant l_{p} in this choice of units has the same numerical value as the resulting intrinsic persistence length (below), and is therefore denoted as l_{p}. The simulations discussed in the following all contain 500 chains of chain lengths in the range $N = 5$ to $N = 200$. A detailed description of all the systems is found in Ref. [8].

3.1. Statics

In polymer melts, excluded volume is commonly assumed to be screened out. Thus, we can expect that polymer chains behave as random walks [27]. This is true at least on large length scales. All *local* interactions only result in local chain stretching. This is seen easily in the single chain static structure factors of model chains [7] (cf. Fig. 5). The random walk appears in the fractal dimension of $d_{\text{f}} = 2$ on

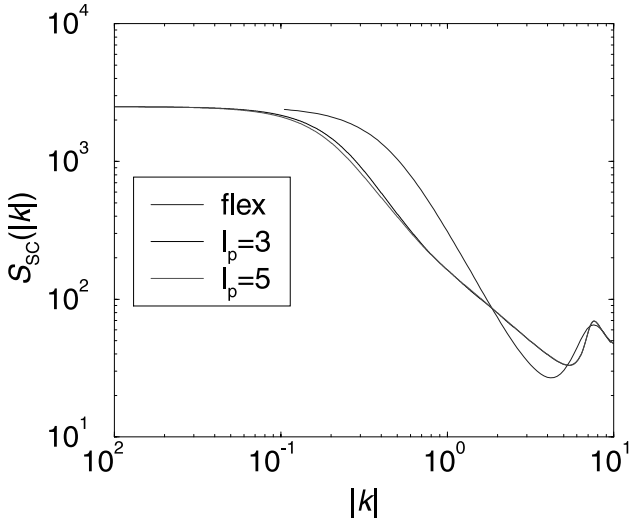

Fig. 5. Static structure factor of model chains of length 50 monomers depending on stiffness. Stiffness is given in terms of the persistence length (see text). 'Flex' means that no stiffening potential is introduced; excluded volume leads to a persistence length of $l_p = 1$.

the length scale larger than the persistence length. The fractal dimension expresses itself in the slope of the structure factor. The chains with stiffness bend over to a weaker slope indicating a smaller fractal dimension at higher $|k|$. The persistence length l_p originates from the Kratky–Porod worm-like chain picture [31]; l_p measures the decay length of bond correlations along the chain backbone. Thus, static properties of different models and chains are easily mapped onto each other by the simple *blob* concept where all local interactions are put into one single length scale, which then allows a renormalization onto flexible chains with the blobs acting as coarse-grained monomers. The size of the Kuhn blob l_K and the persistence length l_p differ only by the constant factor of 2 although they arise from different concepts.

Still, even in chains of complete flexibility, i.e. no three-body potential, there is a small but visible alignment between neighboring chains, similar to that shown in Figs. 3 and 6 on the length scale of about three chain diameters [24]. This is evidence that the very simple ansatz of model chains only incorporating connectivity comes to its limits as soon as many-body interactions become important. As we have seen in Section 2, local interactions strongly affect the mutual packing of chains. If chain stiffness is increased, chain order becomes stronger [7] (cf. Fig. 6) without leading to an overall nematic order. This ordering is a strictly local phenomenon, proven by the fact that there is no chain length dependence whatsoever [24].

3.2. Dynamics

For simple flexible bead-spring chains, the reptation concept was successfully validated by several simulations [22,23,25]. However, NMR experiments of polymer reorientation show that this model cannot describe all polymers satisfactorily. For poly-(dimethylsiloxane), PDMS, which is known to be very flexible, the results of double quantum NMR can be explained by the simple reptation model [32] whereas for polybutadiene this simple explanation shows strong deficiencies [11]. For this purpose, the dependence on stiffness of the reorientation behavior of entangled melts was investigated [8]. With increasing stiffness the reorientation slows down tremendously going hand in hand with a decreasing entanglement length and shrinking tube diameter [10]. The reorientation of backbone segments is algebraic on short time scales (cf. Fig. 7). This algebraic dependence $C_{reor} \propto t^{-\gamma}$ is the same as found in NMR experiments. The exponents of $\gamma = 1/4$ and $\gamma = 1/2$ as seen in Fig. 8 are both found. However, there is a *qualitative* change in dynamics with chain length as the entanglement length is crossed. The

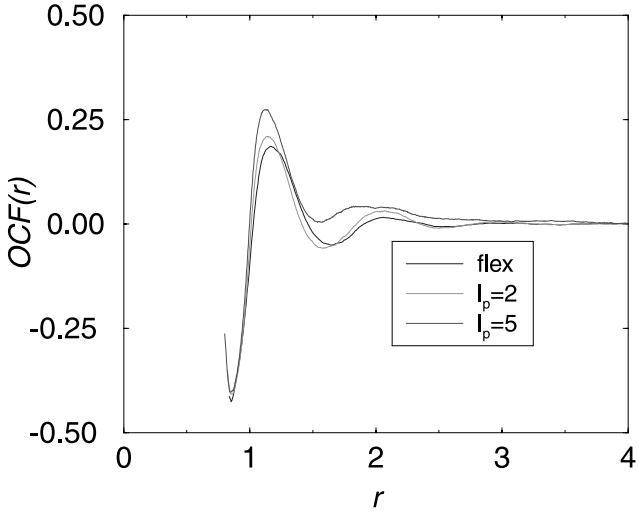

Fig. 6. Static mutual chain packing of chains of different stiffness described by OCF(r) (compare Eq. (1)). The stiffer chains order more strongly parallel. Long range isotropy is preserved (OCF $\to 0$, $r \to \infty$).

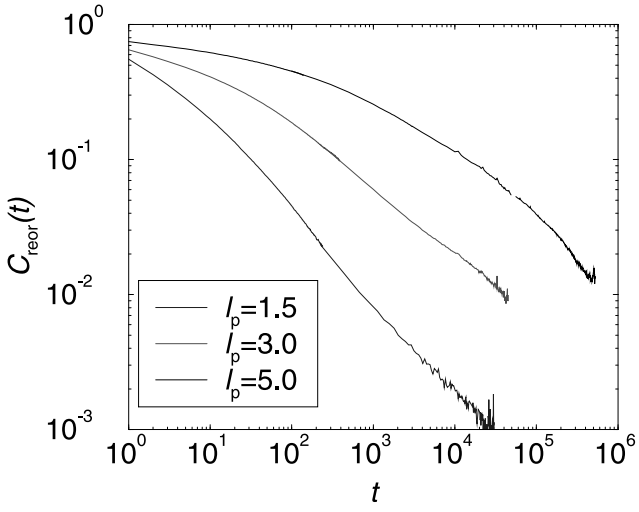

Fig. 7. Algebraic reorientation of segments of the chain backbone depending on chain stiffness (chain length: 200 monomers).

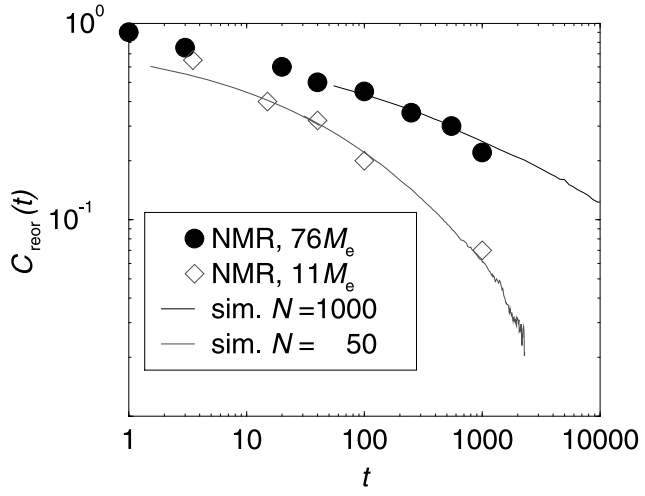

Fig. 8. Comparison of simulated (chains of length 200 and $l_p = 5$; lines) and experimental (symbols) [11] reorientation correlation functions. For the experiments time–temperature superposition is assumed.

exponent of $\gamma = 1/4$ is not found in unentangled chains. In diffusion, the entanglement length scale is also found. Chains longer than l_e diffuse clearly slower than predicted by simple Rouse motion (Fig. 9). According to the Rouse model, the overall diffusion is expected to be $D \propto N^{-1}$. This would correspond to a horizontal straight line in Fig. 9. Reptation leads to $D \propto N^{-2}$ which we find for longer chains. The crossover point can be taken as a definition for the entanglement length [10,22] (Table 2). We observe that the entanglement length *decreases* with increasing persistence length. l_e and l_p are neither independent nor linearly dependent on each other. This makes it impossible to renormalize stiff chains onto the simple bead-spring model, as only one length scale could be scaled away. The influence of stiffness *survives* on very long length scales.

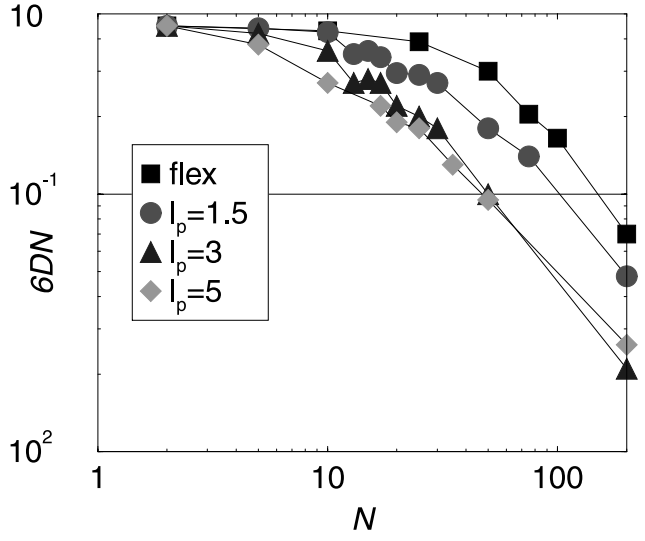

Fig. 9. Diffusion coefficient of chains depending on chain length and stiffness. In the given representation Rouse behavior would give a straight horizontal line.

Table 2
Entanglement monomer number N_e depending on persistence length l_p, determined by the change of diffusion behavior with chain length [10]

l_p	N_e
1	32
1.5	15
3	8
5	6

The entanglement length l_e describes the anisotropy of motion of a chain due to the temporary network of its uncrossable neighbors. A polymer chain has to move predominantly along its backbone as transversal motion is hindered by its neighbors, leading to an effective tube (cf. Fig. 10). This is measured by the correlation of directions of the chain (static $\vec{u}(\tau)$) with the motion of the monomer in time (dynamic $\vec{v}(t - t_0)$) [9,10]

$$\prod(t) = \left\langle \frac{1}{2}[3\vec{u}(\tau)\vec{v}(t - t_0)] \right\rangle \tag{4}$$

This function measures the correlation between the *static* direction of a chain segment at a given point in time with the direction of its *dynamic* motion in the time thereafter. Thus, it shows that chain segments move in the beginning preferably along their contour. This is exactly what reptation is about. Increasing stiffness supports this effect because the stiffness suppresses the transversal motion even further. On short time-scales, where in the standard reptation picture isotropic motion is still possible, the local stiffness disallows this motion. Thus, the chains have to reptate from the very beginning. This is illustrated by the mean-squared displacements of inner monomers ($\langle x^2 \rangle$ cf. Fig. 11). According to the standard reptation picture one expects the scenario we find here only for flexible chains. On short time-scales a Rouse motion [28] is found ($\langle x^2 \rangle \propto t^{0.5}$), then the Rouse motion is constrained to the tube ($\langle x^2 \rangle \propto t^{0.25}$). After the internal

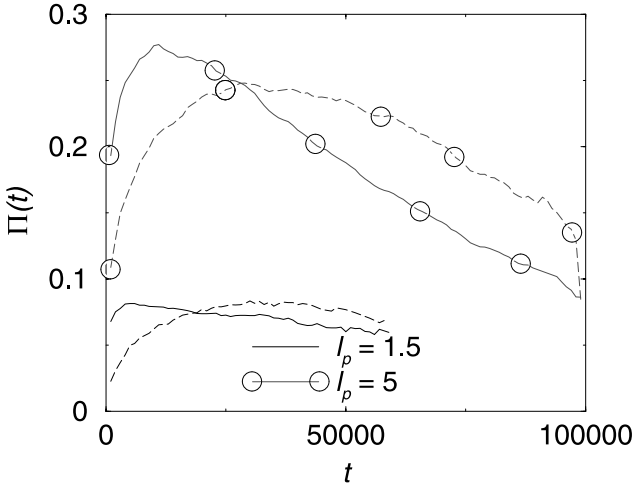

Fig. 10. Correlations of monomer motion with the direction of the backbone depending on stiffness. Solid lines: $t = t_0$, dashed lines $t = t_0 + \tau/2$.

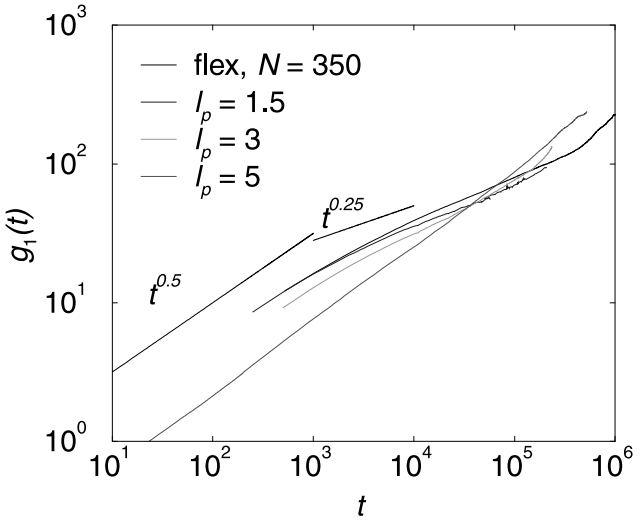

Fig. 11. Mean squared displacements of central monomers in a chain depending on chain stiffness. For clarity lines indicating the slopes corresponding to $t^{0.25}$ and $t^{0.5}$ are shown additionally.

degrees of freedom are relaxed, the chain as a whole moves in the tube ($\langle x^2 \rangle \propto t^{0.5}$) and finally the chains reach free diffusion ($\langle x^2 \rangle \propto t$). The other extreme we now see for chains with a persistence length of five monomers. The first two dynamical regimes are missing completely, as the Rouse motion is no longer the correct description of the polymer especially on short time and length scales (see Fig. 12). This regime we like to call *strong reptation*. Similar results have been obtained by Morse [33–35] for chains of stronger stiffness, who introduced the terms *loosely entangled* and *strongly entangled* for the different systems, respectively.

Note the intersections of the different curves in Fig. 11. This shows that there are regimes where stiffer chains diffuse even faster as the entanglement length and tube diameter come down tremendously. This can also be seen if we look at dynamical structure factors [10] which can measure the tube diameter.

If the Rouse model was applicable in all sub-figures of Fig. 12, all curves would coincide in that scaling as the

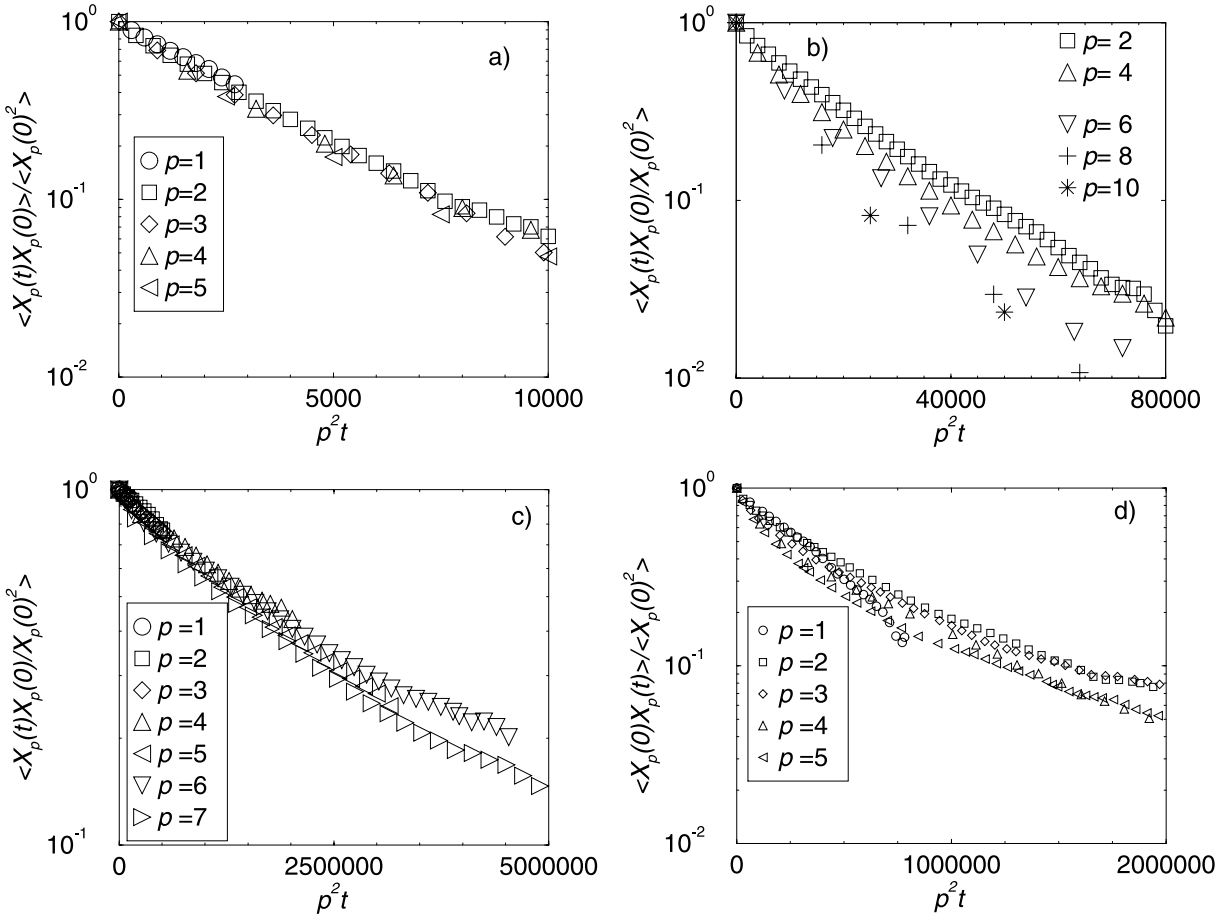

Fig. 12. Normalized correlation functions of Rouse modes X_p of stiff and flexible chains of various stiffnesses: (a) 1–50; (b) 3–50; (c) 5–200; (d) 1–350). The notation means $l_p - N$ with persistence length and chain monomer number. The Rouse model breaks down with increasing length and stiffness.

Rouse modes

$$\vec{X}_p = \frac{1}{N}\sum_{i=0}^{N-1}\cos\left(\frac{\pi p(i+1/2)}{N}\right)\vec{R}_i \quad (5)$$

with $\vec{R}_i$ the position of bead i and N the monomer number, would be the true eigenmodes of the system. However, we see that with increasing stiffness and chain length the model shows deficiencies. Because of stiffness the high modes (local motion) start to be affected and for long chains the entanglements hinder the low modes (large scale motion). As the entanglement length shrinks with stiffness, the region of validity of the Rouse regime vanishes between the entangled motion on the one side and the local stiffness on the other.

4. Conclusions: stiffness — a decisive characteristics

Two different polymer models were introduced. A bead-spring model with stiffness and a fully detailed atomistic model. Both are validated against different experiments. The connecting link between the models is the backbone stiffness which survives from the very local scale to the global scale, in which often only entanglements are expected to be important. In Fig. 13 one sees the success of the mapping. The atomistic chains at 413 K and model chains (both of length 10) are compared (one monomer to one monomer mapping). The mapping is accomplished by rescaling (squared) lengths with the mean-squared end-to-end distance. Time-scales are fixed by the center-of-mass diffusion. Then the figure shows the comparative reorientation of local monomer-to-monomer vectors. Thus, this study opens one possible route to polymer coarse graining. First, simulate an atomistic melt (of oligomers) in full detail; there all the very local observables (sub-monomer to monomer-scale) can be investigated: radial distribution functions, orientation correlations, even structure functions and reorientation times. Also one has to determine the persistence length of the polymer on this scale. This is then taken as an input to the model on the next length scale, so that part of the polymer identity is preserved and a tremendous simulation speedup is possible at the same time. At this scale, long-time dynamic phenomena (e.g. reptation) and large-scale static structure such as the overall Gaussian random walk distribution can be examined.

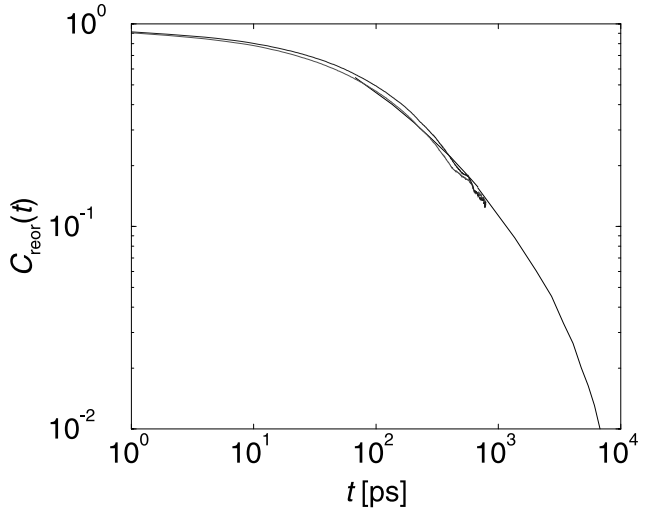

Fig. 13. The reorientation of atomistic chains and simple chains (both of length 10 monomers) in comparison. On the left hand side the lower (C_1) and the upper (C_2) line are atomistic vectors connecting the indicated monomers. The line on the right hand side (continuing the other two lines nicely) corresponds to the simple model with persistence length $l_p = 1.5$ similar to the persistence length of the polyisoprene model. To suppress end-effects the terminal carbons were not taken into account.

However, one has to be very careful with this mapping. There are polymers for which this route is too simple-minded, especially if the monomer is strongly anisotropic or has special or bulky side-groups. More elaborate methods have to be applied in those cases [1,4]. Our method can be applied to dense melts of simple hydrocarbon polymers and allows in this case a very strong speedup and a look at real large-scale phenomena. With the other methods typically an intermediate scale between the two presented scales here is introduced as additional length scales can become important. Still, for dynamic issues it is not possible even on the largest scale to explain everything with simple chains only, at least stiffness has to be taken into account.

Acknowledgements

Many fruitful discussions with Markus Deserno, Burkhard Dünweg, Ralf Everaers, Andreas Heuer, Kurt Kremer, Heiko Schmitz and Doros Theodorou gave valuable ideas to our work. We thank Kevin van Workum for a critical reading of the manuscript. Additionally, financial support by the German Ministry of Research (BMBF) and by the TMR program of the European Union (Contract No. ERBFMRXCT980176) is gratefully acknowledged.

References

[1] Tschöp W, Kremer K, Batoulis J, Bürger T, Hahn O. Simulation of polymer melts. I. Coarse-graining procedure for polycarbonates. Acta Polym 1998;49(2–3):61.
[2] Tschöp W, Kremer K, Hahn O, Batoulis J, Bürger T. Simulation of polymer melts. II. From coarse-grained models back to atomistic description. Acta Polym 1998;49(2–3):75.
[3] Baschnagel J, Binder K, Doruker P, Gusev AA, Hahn O, Kremer K, Mattice WL, Müller-Plathe F, Murat M, Paul W, Santos S, Suter UW, Tries V. Bridging the gap between atomistic and coarse-grained models of polymers: status and perspectives. Adv Polym Sci 2000;152:41.
[4] Meyer H, Biermann O, Faller R, Reith D, Müller-Plathe F. Coarse graining of nonbonded interparticle potentials using automatic simplex optimization to fit structural properties. J Chem Phys 2000;113(15):6264.
[5] Reith D, Meyer H, Müller-Plathe F. Mapping atomistic to coarse-grained

polymer models using automatic simplex optimization to fit structural properties. Macromolecules 2001;34(7):2335.
[6] Faller R, Müller-Plathe F, Doxastakis M, Theodorou D. Local structure and dynamics in *trans* polysisoprene. Macromolecules 2001;34(5):1436.
[7] Faller R, Kolb A, Müller-Plathe F. Local chain ordering in amorphous polymer melts. Influence of chain stiffness. Phys Chem Chem Phys 1999;1(9):2071.
[8] Faller R, Müller-Plathe F, Heuer A. Local reorientation dynamics of semiflexible polymers in the melt. Macromolecules 2000;33(17):6602.
[9] Faller R. Influence of chain stiffness on structure and dynamics of polymers in the melt. PhD Thesis. MPI für Polymerforschung and Universität Mainz, 2000, published at http://archimed.uni-mainz.de/pub/2000/0063.
[10] Faller R, Müller-Plathe F. Chain stiffness intensifies the reptation characteristics of polymer dynamics in the melt. Chem Phys Chem 2001;2(3):180.
[11] Graf R, Heuer A, Spiess H. Chain-order effects in polymer melts probed by ^{1}H double-quantum NMR spectroscopy. Phys Rev Lett 1998;80(26):5738.
[12] Müller-Plathe F, Schmitz H, Faller R. Molecular simulation in polymer science: Understanding experiments better. Prog Theor Phys Kyoto Suppl 2000;138:311.
[13] Pant PVK, Theodorou DN. Variable connectivity method for the atomistic Monte Carlo simulation of polydisperse polymer melts. Macromolecules 1995;28(21):7224.
[14] Mavrantzas VG, Boone TD, Zervopoulou E, Theodorou DN. End-bridging Monte Carlo: a fast algorithm for atomistic simulation of condensed phases of long polymer chains. Macromolecules 1999;32(15):5072.
[15] Dejean de la Batie R, Lauprêtre F, Monnerie L. Carbon-13 NMR investigation of local dynamics at temperatures well above the glass-transition temperature. 3. *cis*-1,4-Polybutadiene and *cis*-1,4-polyisoprene. Macromolecules 1989;22(1):122.
[16] Denault J, Prud'homme J. Carbon-13 nuclear overhauser effect and molecular motion in bulk elastomers. Macromolecules 1989;22(3):1307.
[17] Zorn R, Richter D, Farago B, Frick B, Kremer F, Kirst U, Fetters LJ. Comparative-study of the segmental relaxation in polyisoprene by quasi-elastic neutron-scattering and dielectric-spectroscopy. Physica B 1992;180/181(Part A):534.
[18] Moe NE, Ediger MD. Molecular dynamics computer simulation of local dynamics in polyisoprene melts. Polymer 1996;37(10):1787.
[19] Moe NE, Ediger MD. Calculation of the coherent dynamic structure factor of polyisoprene from molecular dynamics simulations. Phys Rev E 1999;59(1):623.
[20] Grest GS, Kremer K. Molecular dynamics simulation for polymers in the presence of a heat bath. Phys Rev A 1986;33(5):R3628.
[21] Rigby D, Roe R-J. Molecular dynamics simulation of polymer liquid and glass. II. Short range order and orientation correlation. J Chem Phys 1988;89(8):5280.
[22] Kremer K, Grest GS. Dynamics of entangled linear polymer melts: a molecular-dynamics simulation. J Chem Phys 1990;92(8):5057.
[23] Dünweg B, Grest GS, Kremer K. Molecular dynamics simulations of polymer systems. In: Whittington SG, editor. Numerical methods for polymeric systems, vol. 102 of IMA volumes in mathematics and its applications. Berlin: Springer, 1998. p. 159–96.
[24] Faller R, Pütz M, Müller-Plathe F. Orientation correlations in simplified models of polymer melts. Int J Mod Phys C 1999;10(2/3):355.
[25] Pütz M, Kremer K, Grest GS. What is the entanglement length in a polymer melt? Europhys Lett 2000;49(6):735.
[26] de Gennes P-G. Reptation of a polymer chain in the presence of fixed obstacles. J Chem Phys 1971;55(2):572.
[27] Doi M, Edwards SF. The theory of polymer dynamics, vol. 73 of international series of monographs on physics. Oxford: Clarendon Press, 1986.
[28] Rouse PE. A theory of linear viscoelastic properties of dilute solutions of coiling polymers. J Chem Phys 1953;21(7):1272.
[29] Kuhn W. Über die Gestalt fadenförmiger Moleküle in Lösungen. Kolloid Z 1934;68(1):2.
[30] Micka U, Kremer K. Persistence length of weakly charged polyelectrolytes with variable intrinsic stiffness. Europhys Lett 1997;38(4):279.
[31] Kratky O, Porod G. Röntgenuntersuchung gelöster Fadenmoleküle. Recl Trav Chim Pays Bas 1949;68:1106.
[32] Callaghan PT, Samulski ET. The molecular weight dependence of nuclear spin correlations in entangled polymeric liquids. Macromolecules 1998;31(11):3693.
[33] Morse DC. Viscoelaticity of concentrated isotropic solutions of semiflexible polymers. 1. Model and stress tensor. Macromolecules 1998;31(20):7030.
[34] Morse DC. Viscoelaticity of concentrated isotropic solutions of semiflexible polymers. 2. Linear response. Macromolecules 1998;31(20):7044.
[35] Morse DC. Viscoelasticity of tightly entangled solutions of semiflexible polymers. Phys Rev E 1998;58(2):R1237.